Uzbekistan Journal of Polymers
journal homepage: https://uzpolymerjournal.com/
ISSN (online): 2181-3256 (print) 2181-3248

PREPARATION AND CHARACTERIZATION OF OXIDIZED NANOCELLULOSE: STRUCTURAL AND RHEOLOGICAL PROPERTIES

Fayruza M. Urishova[1], Makhliyo M. Kuzieva[1], Dilnavoz G. Batirova [1], Abdumutolib A. Atakhanov [1], Nurbek Sh. Ashurov[1], Dmitriy I. Shiman[2]

[1] Institute of Polymer Chemistry and Physics, Uzbekistan, Tashkent, St. Abdulla Kadyri 7"b"
[2] Research Institute for Physical Chemical Problems of the Belarusian State University, Minsk, Belarus

ARTICLE INFO

Received:22 April 2026
Revised: 28 April 2026
Accepted: 06 May 2026

Keywords:
microcrystalline cellulose, oxidized nanocellulose, potassium permanganate, hydrogels, electrospinning.

Corresponding author
urishovafayruza600@gmail.com

ABSTRACT

The use of potassium permanganate ($KMnO_4$) as an oxidizing agent provides a relatively straightforward yet effective route for tailoring the structure of cellulose under acidic conditions. In this work, microcrystalline cellulose (MCC) was subjected to $KMnO_4$ oxidation to obtain oxidized nanocellulose (ONC), and the transformation is quite evident both structurally and functionally. The oxidation process led to a noticeable decrease in crystallinity (from about 79% in MCC to nearly 59% in ONC), which suggests that not only amorphous regions were affected, but also parts of the ordered domains were partially disrupted. At the same time, fragmentation of cellulose from micro- to nanoscale dimensions was observed, which is important for increasing surface activity and reactivity. Spectroscopic analyses, including FTIR and UV–Vis, confirmed the successful incorporation of carboxyl groups, while XRD results pointed to a partial loss of the native cellulose I structure. Interestingly, the degree of oxidation varied depending on synthesis time, reaching around 18.58% and 9.3% for 480 and 600 minutes, respectively, although this trend seems a bit non-linear and could deserve further clarification. Particle size measurements obtained via dynamic light scattering and atomic force microscopy indicated nanoscale features in the range of roughly 100–220 nm, which aligns well with expected nanocellulose dimensions.
The oxidized nanocellulose displayed pronounced gel-forming ability in alkaline media. Rheological measurements demonstrated typical non-Newtonian behavior, with the storage modulus (G′) exceeding the loss modulus (G″) across a broad range of deformation amplitudes and frequencies, indicating predominantly elastic properties. Depending on the processing conditions, ONC-based materials were successfully fabricated in several forms, including powders, hydrogels, cryogels, films, and nanofibers. The obtained materials exhibit promising potential for applications in polymer composites, hydrogel systems, and other advanced functional materials.

DOI: *10.66640/UJP-2026-5-00007*

Introduction

Cellulose is the most abundant natural polymer on Earth and has long attracted significant scientific and industrial interest due to its renewability, biodegradability, biocompatibility, and versatile chemical structure [1]. The presence of multiple hydroxyl groups in its macromolecular backbone enables cellulose to undergo various chemical modifications, allowing the preparation of

functional derivatives with tailored physicochemical properties. Among the different forms of cellulose, MCC, produced by partial acid hydrolysis of native cellulose, is widely used in pharmaceutical, food, and materials applications owing to its high purity, mechanical stability, and relatively high degree of crystallinity [2,3].

In recent years, nanocellulose-based materials have gained considerable attention as promising building blocks for advanced polymer systems. The transformation from micro- to nanoscale structures leads to a marked increase in specific surface area, enhanced surface reactivity, and improved interfacial interactions with polymer matrices and solvents. As a result, nanocellulose has emerged as a versatile platform for the design of hydrogels, films, adsorbents, composite materials, and biomedical systems.[4].

One of the most effective strategies for producing functional nanocellulose involves chemical oxidation, which introduces reactive functional groups such as carbonyl and carboxyl moieties into the cellulose structure. ONC generally demonstrates enhanced dispersibility in aqueous systems, increased surface charge density, and a greater capacity to form physical and chemical networks. Among the oxidation strategies reported to date, TEMPO-mediated oxidation has been widely investigated owing to its high selectivity for the primary hydroxyl groups at the C6 position of cellulose. [5,6,7]. However, the TEMPO-based system often requires relatively expensive reagents, multicomponent catalytic systems, and precise control of reaction conditions, which may limit its large-scale applicability [8].

In this context, potassium permanganate ($KMnO_4$) represents a strong and readily available oxidizing agent whose reactivity strongly depends on the pH of the reaction medium [9]. Under acidic conditions, permanganate ions are reduced to Mn^{2+} species, enabling effective oxidation of primary hydroxyl groups in cellulose. Compared with TEMPO-mediated systems, $KMnO_4$ oxidation offers several potential advantages, including simpler reaction conditions, lower reagent cost, and the possibility of achieving relatively high oxidation degrees at moderate temperatures. Nevertheless, systematic investigations of the synthesis, structure, and physicochemical properties of ONC obtained via potassium permanganate oxidation remain relatively limited [10].

Furthermore, the ability of oxidized nanocellulose to form structured materials such as gels, films, cryogels, and fibrous networks further broadens its potential applications in advanced functional materials, including adsorption systems, responsive hydrogels, and polymer composites [11].

In recent years, nanofiber materials have attracted significant attention due to their unique physicochemical properties, including a high surface-area-to-volume ratio, tunable porosity, and enhanced mechanical performance. These characteristics make nanofibers promising candidates for applications in filtration, tissue engineering, drug delivery, sensors, and advanced composite materials [14]. Despite extensive studies on electrospinning of synthetic polymers such as polyacrylamide (PAA), polyacrylonitrile (PAN), and polyvinyl alcohol (PVA), as well as natural polymers including cellulose derivatives, the formation of nanofibers from complex polymer systems combining natural and synthetic components remains relatively insufficiently explored.

In particular, the development of stable nanofibers based on oxidized nanocellulose and water-soluble synthetic polymers via electrospinning, together with the investigation of their structural characteristics and intermolecular interaction mechanisms, represents an important research direction [15]. In this study, composite nanofibers were fabricated from a polymer system consisting of polyacrylamide (PAA) and oxidized nanocellulose using the electrospinning technique. The crystalline structure of the obtained nanofibers was analyzed by X-ray diffraction (XRD), while molecular structural changes and intermolecular interactions were examined using Fourier-transform infrared (FTIR) spectroscopy. The obtained results contribute to understanding the interaction mechanisms between ONC and PAA and provide insight into the formation process of composite nanofibers.

The novelty of this work lies in the use of potassium permanganate as an alternative oxidizing agent for the preparation of oxidized nanocellulose with controlled structural properties and its

subsequent incorporation into electrospun composite nanofibers with polyacrylamide. The study establishes relationships between oxidation-induced structural changes in cellulose, rheological behavior of ONC dispersions, and the formation of electrospun nanofibers, providing new insight into the design of nanocellulose-based composite materials.

Materials and methods

2.1. Materials

Microcrystalline cellulose (MCC) was used as the starting cellulose source [16]. Potassium permanganate ($KMnO_4$), sulfuric acid (H_2SO_4), hydrogen peroxide (H_2O_2), polyacrylamide (Praestol™ 2500 PAA), and sodium hydroxide (NaOH) were purchased from Sigma-Aldrich and used as received without further purification.

2.2 Methods

Oxidation of microcrystalline cellulose with potassium permanganate.

Microcrystalline cellulose was oxidized with $KMnO_4$ in an acidic medium. First, 360 ml of 1% dilute sulfuric acid was poured into a three-necked flask covered with aluminium foil. 5 g of MCC and 3.85 g of potassium permanganate were added to the flask with stirring, and the reaction was continued at 40°C for 160,240 minutes. After the reaction was completed, 5 ml 30% hydrogen peroxide was added to convert MnO_2 to colorless Mn^{2+}. The ONC system immediately turned white and the reaction was stopped. The above suspension was filtered and washed with distilled water, dispersed by ultrasound for 10 minutes, and then centrifuged 3 times. The resulting gel-like mass was dried by lyophilization.

Determination of Carboxyl Content

The oxidation degree of the samples was determined using the calcium acetate method, with slight modifications based on the procedure described in the United States Pharmacopoeia. Briefly, 0.4 g of the oxidized sample (previously dried to constant weight) was accurately weighed and transferred into a glass-stoppered flask. The sample was then treated with 20 mL of a 0.25 M aqueous calcium acetate solution $Ca(CH_3COO)_2$ and allowed to react for approximately 7 hours at room temperature under static conditions.

After completion of the reaction, the mixture was titrated with a standardized 0.05 N NaOH solution to determine the amount of liberated acetic acid. The carboxyl group content was then calculated using the following equation [18].

$$COOH = \frac{N \cdot V \cdot MW_{(COOH)}}{m} \cdot 100$$

where N is the normality of 0.1 M NaOH solution; V is the consumed volume of NaOH which is corrected for the blank solution; MWCOOH is the molecular weight of the carboxyl group.

Preparation and Rheological Study of ONC Hydrogels

The rheological measurements were carried out using a MCR 302 Anton-Paar rheometer (Gratz, Austria) equipped with plane geometry of 50 mm diameter, for the selected gap of 500 μm. ONC hydrogels were prepared by dispersing ONC in aqueous sodium hydroxide solution followed by freeze–thaw cycles. Rheological properties were studied using amplitude and frequency sweep tests to determine storage modulus (G′), loss modulus (G″), viscosity behavior, and yield stress.

Preparation of ONC Cryogels

Cryogels based on oxidized nanocellulose (ONC) were prepared via a freezing–lyophilization method. The pre-formed ONC hydrogel was transferred into molds and subjected to freezing at temperatures ranging from −20 °C to −60 °C for 12–24 h. During the freezing process, ice crystals

formed within the hydrogel matrix and acted as porogens, inducing phase separation and facilitating the development of a three-dimensional interconnected network structure.

Formation of nanofibers based on ONC by electrospinning

The formation of nanofibers was carried out by the electrospinning equipment NanoNC eS-robots (South Korea). The electrospinning conditions were as follows: applied voltage 25 kV, needle tip and collector distance 14 cm; needle diameter 0.353 mm; injection solution flow rate 45 μl/min; relative humidity 60%, temperature 250C.

FTIR

The FTIR spectrometer "Inventio-S" (Bruker) was used and FTIR spectra were recorded in 400–4000cm^{-1}wavenumber range with a resolution of 2 cm^{-1} and 32 scans at a temperature of 25°C. All samples were finely ground, dried at 60°C for 12 h, and pressed into KBr pellets (1 wt%) before analysis. Soft-ware of OPUS was applied to determine the peaks at specific points.

Ultraviolet (UV) Spectroscopy

UV spectra of samples were recorded with a Specord 210 UV-spectrophotometer (Analytic Jena, Germany) by using quartz cells 1 cm in diameter and 1 nm slit; the scanning range of measurement was 190–1000nm, a scanning speed was 5nm/s. The aqueus ONC suspensions (0.05 wt%) were ultrasonically dispersed for 15 min prior to measurement.

Atomic force microscopy (AFM)

Morphological studies of ONC were performed by using AFM Agilent 5500 (Agilent, USA). The silicon cantilevers with a stiffness of 9.5 N/m^2 were used and the frequency was 262 kHz. The AFM scan area (x – y – z) was 3.0 - 3.0 - 1 μm.

Wide-angle X-ray diffraction

XRD studies were carried out using XRD Miniflex 600 (Rigaku, Japan) with monochromatic CuKα radiation isolated by a nickel filter with a wavelength of 1.5418 Å at 40 kV and the current strength of 15 mA. The spectrum was recorded in the interval 2θ = 5°–40°. The air-dried ONC powders were gently ground, mounted on zero-background glass slides, and analyzed under identical sample thickness and humidity conditions. The data processing of experimental diffraction patterns, peak deconvolution, describing the peaks used by Miller indices, peak shape, and the basis for the amorphous contribution were conducted using the software "SmartLab Studio II" and data base PDF-2 (2020 Powder diffraction file, ICDD)

Dynamic Light Scattering (DLS)

Particle size distribution was measured on a Photocor Compact (Photocor, Russian) at 298 K, using a 635.6 nm semiconductor laser (25 mW). The ONC suspensions were prepared at 0.01 wt%, sonicated for 10min to disperse aggregates, and filtered through a 0.45 μm PTFE membrane before measurement at 25°C.

Results and Discussion

Potassium permanganate is a strong oxidizing agent and, depending on the pH of the solution, it oxidizes various substances and reduces them to manganese compounds with different oxidation states. In an acidic medium - to manganese (II) compounds, in a neutral medium - to manganese (IV) compounds, in a strongly alkaline medium - to manganese (VI) compounds (Figure 1).

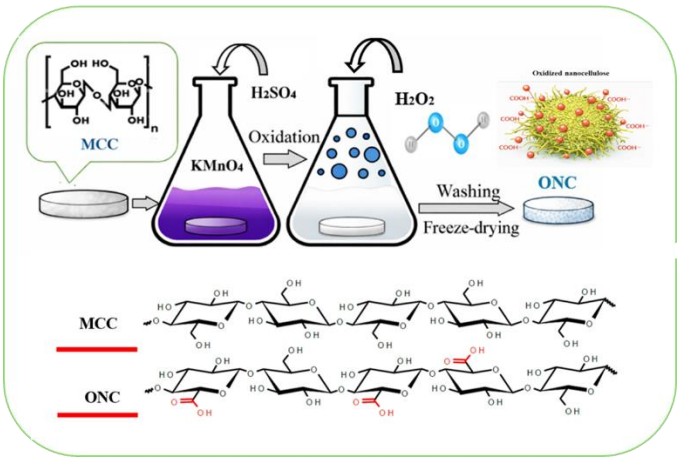

Figure 1. *MCC oxidation reaction mechanism*.

Initially, oxidized nanocellulose (ONC) was synthesized by oxidizing MCC with potassium permanganate in an acidic medium. MCC was dissolved in distilled water under constant stirring to obtain a homogeneous suspension. Sulfuric acid was added to adjust the pH of the system to the desired value. Then, the potassium permanganate solution was slowly introduced into the suspension with constant stirring. The obtained ONC was separated by centrifugation, repeatedly washed with distilled water until a neutral pH was reached, and further purified by dialysis to remove residual ions [18]. The purified product was dried or stored as an aqueous dispersion, depending on further use. It can be concluded that in this oxidation system, MnO_4^- is converted to Mn_2^+ by the C6-OH unit of cellulose [19]. The excess MnO_4^- ion participates in the oxidation of Mn_2^+ to colloidal MnO_2, which is a self-catalyst and provides the system with a high oxidation rate. The acidic environment helps to maintain $KMnO_4$ in the Mn^{7+} state and ensures efficient oxidation. Sulfuric acid (H_2SO_4) is usually used to provide the desired acidic pH environment. It also helps control the oxidation rate, preventing excessive oxidation of cellulose to carbon dioxide and water. ONC samples exhibited a progressive increase in carboxyl group content with increasing oxidation time. The samples obtained after 160 and 240 minutes contained 18.58% (4.13 mmol/g) and 9.3% (1.92 mmol/g) of carboxyl groups, respectively (Figure 2). This trend indicates a gradual oxidation of the primary hydroxyl groups at the C6 position during the 160 min oxidation and confirms the efficiency of the oxidation process, while it can be seen that the amount of carboxyl groups decreased during the 240 min oxidation.

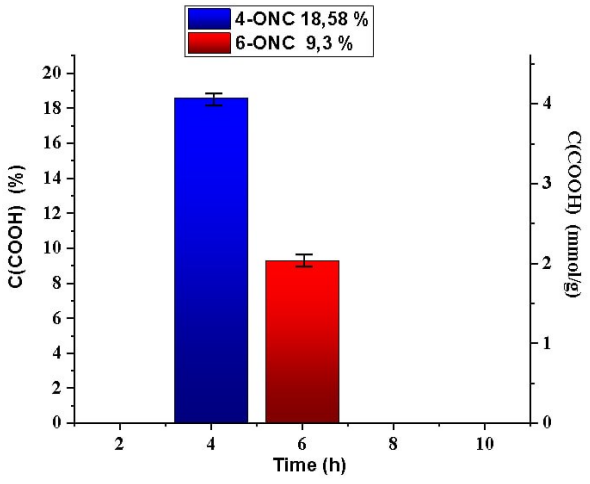

Figure 2. *Dependence of the content of carboxyl groups in ONC samples*

The oxidation process leads to the weakening of intermolecular hydrogen bonds in cellulose chains by the introduction of carboxyl and carbonyl groups. This partially damages the crystalline structure, which leads to the fragmentation of larger microcrystalline cellulose particles into smaller ones, resulting in the formation of nanosized particles (Figure 3).

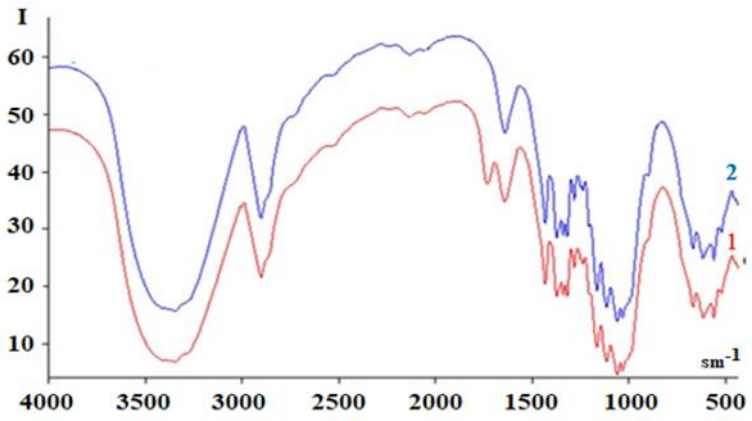

Figure 3. *FTIR spectra of MCC (1) and ONC (2) samples*

The formation of carboxyl groups was confirmed by FTIR spectroscopic studies. Comparative studies of MCC and ONC showed that absorption bands associated with O-H vibrations were observed in the infrared spectra at ~ 3400 cm^{-1}. In the case of ONC, this absorption band narrows and becomes more pronounced due to the reduction in the number of hydroxyl groups participating in hydrogen bonds. Deformational vibrations of the -CH bonds in the methylene groups were observed in the region of 2800-2950 cm^{-1}. In contrast to the spectrum of MCC samples, a new absorption band appeared in the ONC spectra at a wavelength of 1721 cm^{-1}, which is associated with the vibrational vibration of C=O. At the same time, the signal intensity in the 1425 cm^{-1} region associated with the vibrations of the -CH_2- groups decreases, and the intensity of the vibrations associated with the out-of-plane vibrations of the -CH_2- groups increases in the 1315 cm^{-1} absorption zone. It was confirmed that the pyranose ring in the elementary unit of cellulose is preserved, which confirms the oxidation of the C6 hydroxyl group

The formation of carboxyl (-COOH) and carbonyl (C=O) groups during the oxidation process led to the appearance of peaks in new absorption regions in the UV spectrum (Figure 4).

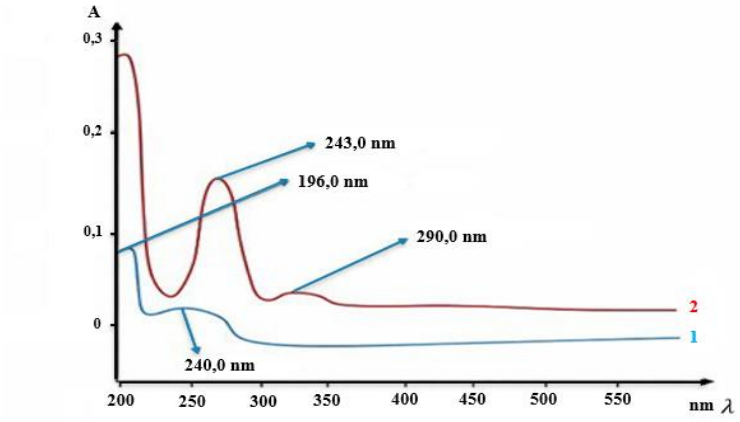

Figure 4. *UV spectra of MCC (1) and ONC (2) samples*

Typically, the π→π* transition of C=O bonds in carboxyl groups occurs in the 190–210 nm region. After oxidation, a low-intensity absorption spectrum can be observed in the absorption spectrum around 200–210 nm, corresponding to the absorption of carboxyl or carbonyl groups introduced during the oxidation process. This is the result of the π→π* transitions of double bonds,

i.e. C=O groups, which are absent in unoxidized microcrystalline cellulose. The 240 nm absorption spectra observed in MCC and ONC are formed as a result of the transition from the ground state of unpaired electrons in the oxygen atoms of hydroxyl groups to the excited state, i.e. n→σ*. The absorption spectra formed in oxidized nanocellulose in the 290 nm region are related to the n→π* electronic transitions in the oxygen atom.

Oxidation of microcrystalline cellulose with potassium permanganate ($KMnO_4$) significantly changes its structure, and these structural changes can be seen in X-ray diffraction analysis (Figure 5).

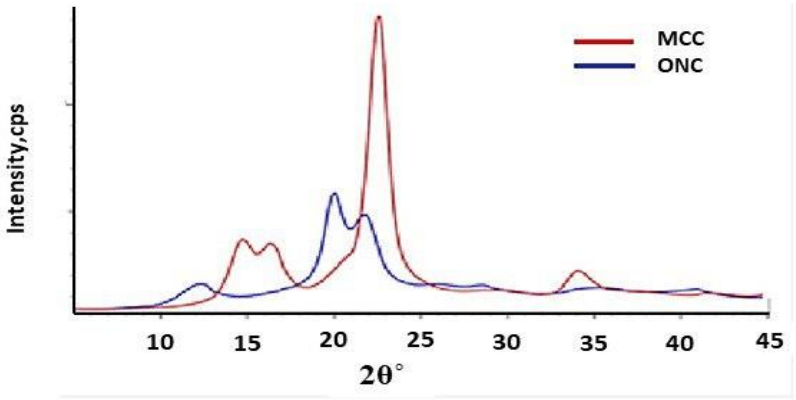

Figure 5. *X-ray diffraction patterns of MCC and ONC*

The mechanism of these changes is based on the oxidation of hydroxyl groups in cellulose chains, especially at the C6 position, to carboxyl groups (-COOH), which affects both crystalline and amorphous regions of cellulose. MCC has an amorphous-crystalline structure consisting of crystalline and amorphous parts. The crystalline regions are well ordered and produce sharp diffraction peaks in the X-ray diffraction pattern. These regions are usually associated with the structure of cellulose I (native cellulose), where the cellulose chains are strongly linked by hydrogen bonds. The amorphous regions are disordered, resulting in broader and less intense peaks in the X-ray diffraction pattern.

In MCC, the cellulose chains are arranged in a highly ordered, rigid structure. In the crystalline regions, the chains interact through strong intermolecular hydrogen bonds between hydroxyl groups (-OH) in adjacent cellulose chains. This ordered structure is the basis for the high degree of crystallinity of MCC (~79%). MCC is primarily composed of cellulose I, a more crystalline form of cellulose with a well-defined order of cellulose chains. This structure exhibits sharp and intense peaks in the X-ray diffraction peaks.

When MCC was oxidized with potassium permanganate, a decrease in the degree of crystallinity from 79% to 59% (in ONC) was observed, which is explained by the distortion of the crystal structure during the oxidation process. This distortion is primarily due to the introduction of carboxyl groups (-COOH) and structural changes associated with the cellulose polymer chains.

During oxidation, hydroxyl groups (-OH), which are involved in the formation of hydrogen bonds between cellulose chains, are replaced by carboxyl groups (-COOH) [20]. Carboxyl groups are more reactive and have a larger spatial volume than hydroxyl groups, which leads to the disruption of some of the hydrogen bonds that maintain the crystal order. When hydrogen bonds are broken and new carboxyl groups are formed, the cellulose chains cannot maintain their ordered structure in the crystalline regions. This leads to the disordering of the crystalline parts, which leads to a decrease in the degree of crystallinity. Oxidation process begins in the amorphous regions of cellulose, where the chains are relatively disordered. As the oxidation process continues, it also affects the ordered crystalline regions. This leads to increase in the total amount of amorphous part of the cellulose structure. The disruption of hydrogen bonds and the formation of new functional groups transform some of the ordered regions into less ordered regions. This is reflected in the

broadening of the X-ray diffraction peaks, especially around 2θ = 18-19°, corresponding to amorphous regions. In oxidized nanocellulose, the sharp peaks associated with the cellulose I crystal structure become weaker and broader due to the loss of order in the crystalline regions. The intensity of the cellulose I peak decreases at 2θ = 22.5° (for the 200 plane), indicating a decrease in the size of the crystalline parts.

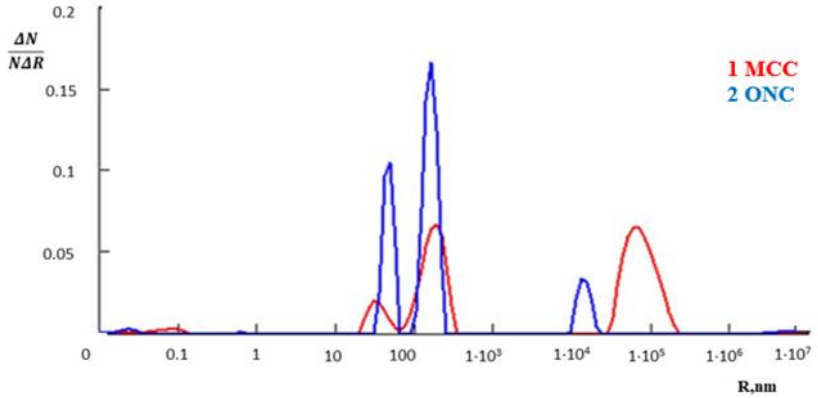

Figure 6. *DLS results of MCC (1) and ONC (2) samples*

The effect of the oxidation process on particle shape and size was evaluated by dynamic light scattering (DLS), which showed a change in particle size from micrometers to nanometers and a polymodal distribution of particles was also observed (Figure 6). A decrease in the size of ONC particles with increasing duration of the oxidation process was also observed in ACM studies (Figure 7).

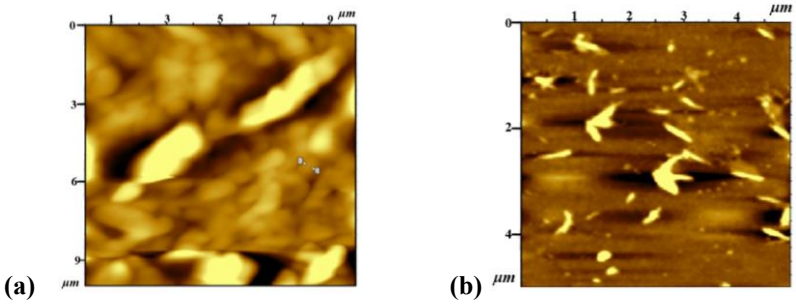

Figure 7. *ACM images of MCC (a) and ONC (b) samples*

ACM studies showed that the size of ONC decreased to 106-180 nm and the shapeless agglomerate particles in MCC samples were observed to have spherical and needle-like shapes.

The possibility of making MCC oxidation more favorable under mild conditions using potassium permanganate in an acidic environment has been demonstrated.

Based on the results obtained, the performance of ONC samples synthesized by two novel methods [21] and obtained by the widely used TEMPO-oxidation method presented in the literature was compared (Table 1).

Table 1

Indicators of ONC samples obtained using different methods

Samples	Particle size	Degree of polymerization	Reaction yield, %
NC	50-500 nm	240	-
MCC	50-450 mkm	350	-
ONC ($K_2Cr_2O_7$)	113-172 nm	172	88
ONC ($KMnO_4$)	180-220 nm	192	93
ONC (TEMPO)	184-230 nm	216	81
ONC(TEMPO/NaClO)	100-300 nm	490	90

The results showed that the proposed ONC samples synthesized by the dichromate and permanganate method [7,13,19] differ from the ONC samples obtained by the TEMPO-oxidation method in terms of higher carboxyl group content, higher reaction yield, and smaller particle size.

The studies conducted revealed that the synthesized ONC samples have gel-forming properties. Sodium hydroxide solution was used in the gelation process. Sodium hydroxide can break the hydrogen bonds between ONC chains, which weakens the intermolecular interactions between ONC and increases the degree of dispersion. This allows the carboxyl groups to interact more effectively with water molecules, leading to better swelling. NaOH can deprotonate the carboxyl groups (-COOH) in oxidized nanocellulose and form carboxyl anions ($-COO^-$). These negatively charged groups enhance the electrostatic interaction between cellulose chains and prevent aggregation. Using the freeze-thaw method, it was possible to obtain ONC hydrogels with high swelling capacity [21].

The properties of the resulting gels were investigated using rheological studies using amplitude and frequency approaches sweep.

Amplitude sweep tests are used to evaluate the deformation behavior of materials within the non-destructive region and to determine the upper limit of the linear viscoelastic range (LVR). In this region, the internal structure remains intact, and the viscoelastic properties do not change with increasing strain or stress. When the applied stress exceeds this limit, structural rearrangement begins, leading to a decrease in rigidity and the onset of softening. With further increase in deformation, the material may start to flow or, depending on its structural strength, retain a predominantly elastic behavior.

In the amplitude-steering method, the amplitude is changed while keeping the frequency constant. In this case, the storage modulus (G') and the loss modulus (G") are controlled. G' is the elastic part of the hyperelastic behavior, which characterizes the behavior of the sample in the solid state. G" is the viscous part of the hyperelastic behavior, which can be considered as the behavior of the sample in the liquid state.

The results showed that for both the permanganate and dichromate methods of ONC samples, the limit of the linear superelastic range is located in the amplitude range of 0.02-0.3%, and it is in this range that the structure of the samples exists in an intact state (Figure 8).

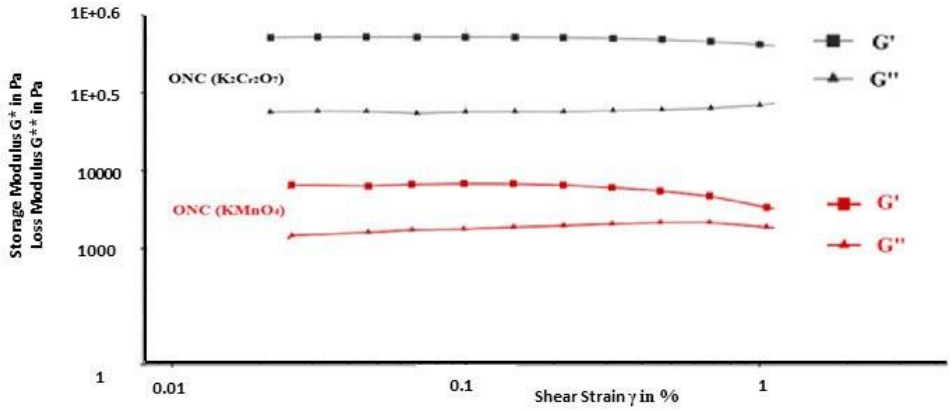

Figure 8. *Rheological measurements of ONC gels by amplitude*

It was found that in the studied range G'>G", that is, the storage modulus is higher than the loss modulus, indicating that the system is in a gel state, and in this case, the values of G' and G" are higher than those of samples obtained by the bichromate method [22].

The frequency-dependent rheological properties of ONC gel samples were carried out in order to determine the time-dependent behavior of the sample in the stress range where the structure is not damaged (Figure 9).

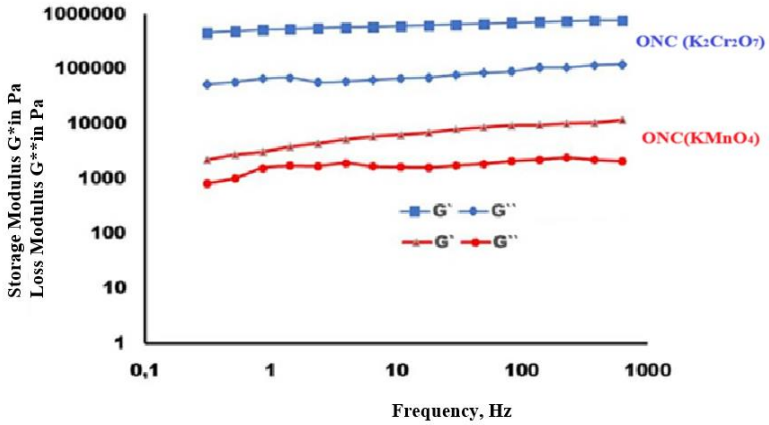

Figure 9. *Frequency-dependent rheological measurements of ONC gels*

Based on the results the ONC samples exhibited properties typical of gels throughout the measured range, with the storage modulus of the samples being higher than the ignition modulus, which was evident up to a frequency of 100 Hz, and in these studies, samples obtained by the bichromate method also had relatively high values.

The viscosity properties of the gels were studied by observing the change in their viscosity under the influence of different shear forces. This makes it possible to determine their yield point, i.e. the transition from a solid to a liquid state.

In the quiescent state, macromolecules form a three-dimensional, ordered stable structure due to various interactions with each other, and the material is in a solid state. When a shear stress is applied to this system, when certain values are reached, this force disrupts the ordered structure and the material begins to flow, that is, passes into a liquid state. The sample begins to flow only if the applied external forces are stronger than the forces of the internal structure of the material, and this value indicates the yield point.

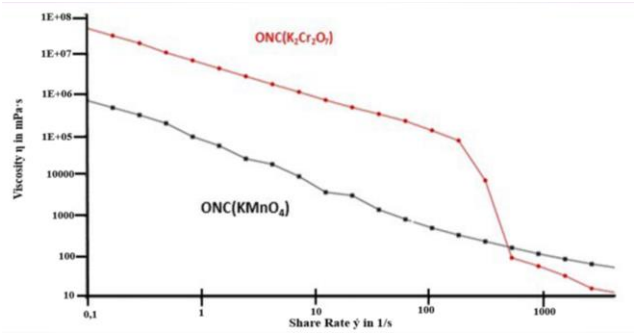

Figure 10*. Viscosity of ONC samples as a function of shear stress*

Rheological studies have shown that the systems (Figure 10) exhibit non-Newtonian fluid behavior. In other words, the decrease in viscosity with increasing shear rate is not constant over the entire range of shear rates. The effect of shear orientation is minimal at low shear rates [23].

The samples have high viscosities, and a decrease in viscosity with increasing shear rate was observed, i.e., these systems exhibited properties typical of non-Newtonian fluids.

Based on the studies, ONC and its derivatives were obtained in four different forms: powder, gel, cryogel (sponge), and film (Figure 11).

Figure 11. *Different forms of ONC: (from left to right) powder; gel; sponge (cryogel)*

Based on preliminary studies, it was found that it is possible to obtain elastic and deformable sponges (cryogels) with a network structure by lyophilizing the formed gels at high low temperatures (-60^{0}C). By drying the gels on a flat surface at temperatures of 40-50^{0}C, mechanically strong elastic films were obtained. Films and sponges may be of interest for use in biomedicine. These objects are planned to be analyzed in more depth in our future studies.

Study of the possibilities of obtaining nanofibers based on oxidized nanocellulose.

Currently, scientific research is developing on the production of nanofibers based on synthetic and natural polymers using the electrospinning method [24]. Unfortunately, there are relatively few works related to complex systems, that is, on the formation of nanofibers based on composites. From this point of view, the scientific significance of solving the problem of obtaining nanofibers from the developed complex systems is undoubtedly high, in which it is important to find optimal conditions for electrospinning nanofibers, determine the structure and a number of special properties, as well as areas of application. The tasks aimed at identifying the production processes for obtaining nanorange fibers based on complex polymer systems using the electrospinning method and determining their areas of application are relevant.

The crystal structure of ONC samples and ONC/PAA nanofibers was evaluated using X-ray diffraction analysis. X-ray diffraction studies showed that in the ONC sample, four crystal domains were observed in the region 2θ = 14º, 16º, 22º and 34º, corresponding to the (101), (10-1), (002) and (040) planes (Figure 12). An amorphous structure was observed in the diffraction lines of ONC/PAA-based nanofibers. This is due to the conditions for obtaining the nanofibers. Pure solutions of ONC and PAA are used to produce ONC/PAA nanofibers.

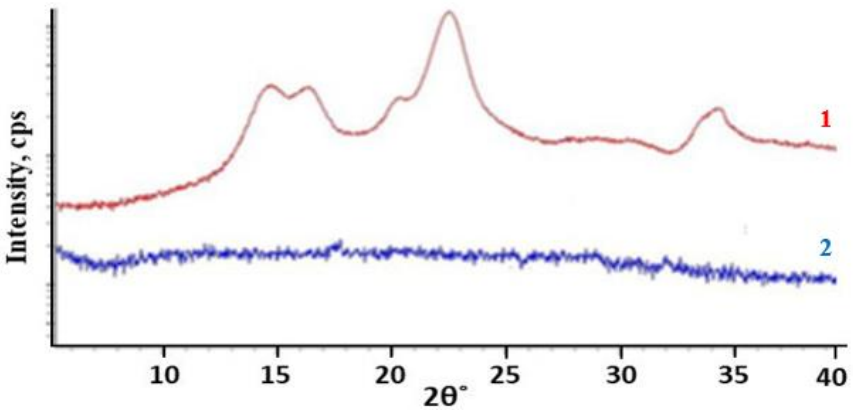

Figure 12. *Diffractogram of ONC (1) and PAA/ONC fibers (2)*

The IR spectra of ONC and ONC/PAA nanofibers show stretching vibrations of hydroxyl groups in the region of 3400 cm^{-1}, corresponding in value to intermolecular and intramolecular hydrogen bonds. At the same time, in nanofibers this absorption line narrows and a peak associated with the amide group of PAA appears. Stretching vibrations of C-H bonds in the methylene and methine groups of cellulose appear in the regions of 2800-2950 cm^{-1}(Figure 13).

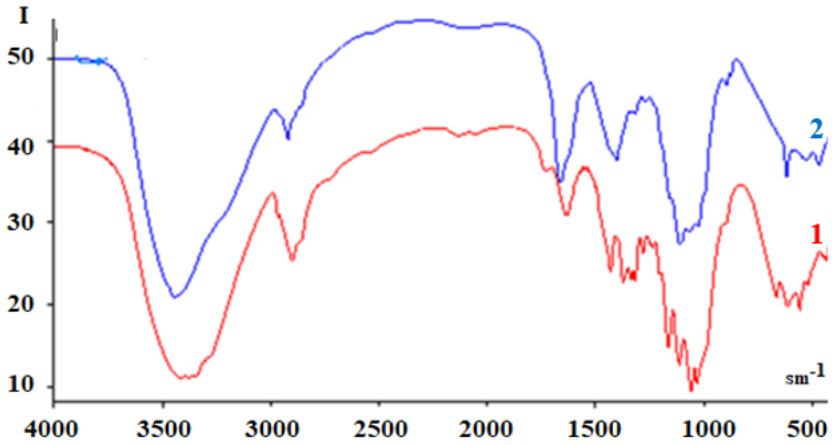

Figure 13. *FTIR spectra of ONC (1) and PAA/ONC fibers (2).*

The vibrations of adsorbed water molecules are observed in the region around 1635 cm^{-1}. The absorption lines in the regions 1420 cm^{-1}, 1335 cm^{-1}, 1337 cm^{-1} and 1202-1058 cm^{-1} correspond to the deformation vibrations of the CH, -CH_2, -OH, -CO groups and the valence vibrations of the C-O group. At the same time, a decrease in the absorption intensity in the regions 3419 cm^{-1}, 2903 cm^{-1} and 1662 cm^{-1} is observed. The peaks located in these absorption regions correspond to the vibrations of C-H, O-H and adsorbed water molecules. Unlike the spectra of ONC samples, the absorption band at 1721 cm^{-1}, which is associated with the C=O stretching vibration of carboxyl groups in nanofibers, is not observed, but the absorption band appears at 1659 cm^{-1}, and all the lines in the wave region of 1420 cm^{-1}, 1335-1375 cm^{-1} correspond to deformation vibrations. Based on the conducted studies, the possibility of forming nanofibers based on PAA captured by ONC using the electrospinning method was demonstrated.

Conclusion

In this study, an efficient and relatively mild approach for the oxidation of microcrystalline cellulose (MCC) using potassium permanganate in an acidic medium was successfully demonstrated, resulting in the formation of oxidized nanocellulose (ONC) with tailored structural and physicochemical properties. The oxidation process predominantly occurred at the C6 primary hydroxyl groups, leading to the introduction of carbonyl and carboxyl functionalities. This chemical modification weakened intermolecular hydrogen bonding and partially disrupted the crystalline structure of MCC, promoting fibrillation and fragmentation of cellulose from the microscale to the nanoscale, yielding ONC particles with sizes in the range of ~100–220 nm and reduced crystallinity. Comparative analysis indicated that ONC obtained via permanganate and dichromate oxidation routes exhibits higher carboxyl group content, improved reaction efficiency, and smaller particle sizes compared to ONC produced by the conventional TEMPO-mediated oxidation method, highlighting the effectiveness of these alternative oxidation strategies.

The synthesized ONC demonstrated pronounced gel-forming ability in alkaline media, enabling the preparation of hydrogels exhibiting typical non-Newtonian rheological behavior with dominant elastic characteristics ($G' > G''$) over a wide range of deformation conditions. Depending on processing conditions, ONC-based materials were successfully fabricated in multiple forms, including powders, hydrogels, cryogels (sponges), films, and electrospun nanofibrous mats. In particular, the incorporation of ONC into electrospinning systems enabled the formation of uniform nanofibers with enhanced structural integrity, surface functionality, and potential for high surface area applications.

Structural and spectroscopic analyses further demonstrated that ONC can be effectively integrated into polymer matrices, leading to the formation of amorphous nanofibrous networks stabilized by intermolecular interactions such as hydrogen bonding and electrostatic interactions. The

combination of tunable surface chemistry, nanoscale morphology, and processability into diverse material formats underscores the versatility of ONC.

Overall, the obtained ONC and its derivatives exhibit strong potential for applications in environmental remediation (adsorption), biomedicine, drug delivery systems, hydrogel-based platforms, and electrospun nanofiber composites. The presented oxidation strategy provides a robust and scalable pathway for the design of multifunctional cellulose-based materials, warranting further investigation toward advanced functional and industrial applications.

Research funding.

This research was supported by the Basic Fundamental Program of the Academy of Sciences of the Re-public of Uzbekistan, and the Uzbekistan–Belarus joint project funded by the Ministry of Higher Education, Science and Innovation of the Republic of Uzbekistan (Grant No. FL-8824063315, X25UZB-126).

REFERENCES

[1]. Shaghaleh, H., Xu, X., & Wang, S. (2018). Current progress in production of biopolymeric materials based on cellulose, cellulose nanofibers, and cellulose derivatives. RSC advances, 8(2), 825-84 https://doi.org/10.1039/C7RA11157F

[2]. Aziz, T., Fan, H., Haq, F., Khan, F. U., Numan, A., Ullah, A., & Wazir, N. (2019). Facile modification and application of cellulose nanocrystals. Iranian Polymer Journal, 28(8), 707-724. https://doi.org/10.1007/s13726-019-00734-2

[3]. 3 Garg, T., Arora, S., & Pahwa, R. (2025). Cellulose and its derivatives: Structure, modification, and application in controlled drug delivery. Future Journal of Pharmaceutical Sciences, 11(1), 76. https://doi.org/10.1186/s43094-025-00834-2.

[4]. 4 Aziz, T., Ullah, A., Ali, A., Shabeer, M., Shah, M. N., Haq, F., ... & Khan, F. U. (2022). Manufactures of bio-degradable and bio-based polymers for bio-materials in the pharmaceutical field. Journal of Applied Polymer Science, 139(29), e52624. https://doi.org/10.1002/app.52624

[5]. 5. Zhang, T., Lang, J., Liu, L., Liu, L., Li, H., Gu, Y., ... & Ding, X. (2017). Effect of carboxylic acid groups on the supercapacitive performance of functional carbon frameworks derived from bacterial cellulose. Chinese Chemical Letters, 28(12), 2212-2218. https://doi.org/10.1016/j.cclet.2017.08.013

[6]. 6. Isogai, A. (2022). TEMPO-catalyzed oxidation of polysaccharides. Polymer Journal, 54(4), 387-402. https://doi.org/10.1038/s41428-021-00580-1

[7]. 7. Isogai, A., Saito, T., & Fukuzumi, H. (2011). TEMPO-oxidized cellulose nanofibers. nanoscale, 3(1), 71-85. https://doi.org/10.1039/C0NR00583E

[8]. 8. Chen, C., Xi, P., Zhang, S., Zhang, L., Sun, Y., Yao, J., ... & Jiang, Y. (2022). Nanocellulose with unique character converted directly from plants without intensive mechanical disintegration. Carbohydrate polymers, 293, 119730. https://doi.org/10.1016/j.carbpol.2022.119730.

[9]. 9 Kao, C. M., Huang, K. D., Wang, J. Y., Chen, T. Y., & Chien, H. Y. (2008). Application of potassium permanganate as an oxidant for in situ oxidation of trichloroethylene-contaminated groundwater: a laboratory and kinetics study. Journal of Hazardous Materials, 153(3), 919-927. https://doi.org/10.1016/j.jhazmat.2007.09.116

[10]. 10. Bragd, P. L., Van Bekkum, H., & Besemer, A. C. (2004). TEMPO-mediated oxidation of polysaccharides: survey of methods and applications. Topics in Catalysis, 27(1), 49-66. https://doi.org/10.1023/B:TOCA.0000013540.69309.46

[11]. 11. Chen, Y., Zhang, L., Yang, Y., Pang, B., Xu, W., Duan, G., ... & Zhang, K. (2021). Recent progress on nanocellulose aerogels: preparation, modification, composite fabrication, applications. Advanced Materials, 33(11), 2005569. https://doi.org/10.1002/adma.202005569

[12]. 12. Zhang, Y., Jiang, S., Xu, D., Li, Z., Guo, J., Li, Z., & Cheng, G. (2023). Application of nanocellulose-based aerogels in bone tissue engineering: current trends and outlooks. Polymers, 15(10), 2323. https://doi.org/10.3390/polym15102323

[13]. 13. Kuzieva, M. M., Urishova, F. M., Atakhanov, A. A., Ashurov, N. S., Rashidova, S. S., Shiman, D. I., ... & Kang, S. (2025). Potassium Permanganate–Oxidized Nanocellulose: Structural Features and Rheological Performance for Advanced Applications. Eurasian journal of chemistry, 30(4 (120)), 148-159. https://doi.org/10.31489/2959-0663/4-25-18

[14]. 14. Li, D., & Xia, Y. (2004). Electrospinning of nanofibers: reinventing the wheel? Advanced materials, 16(14), 1151-1170. https://doi.org/10.1002/adma.200400719

[15]. 15. Bhardwaj, N., & Kundu, S. C. (2010). Electrospinning: A fascinating fiber fabrication technique. Biotechnology advances, 28(3), 325-347. https://doi.org/10.1016/j.biotechadv.2010.01.004

[16]. 16. Saidmuhamedova, M. Q., Turdiqulov, I. H., Atakhanov, A. A., Ashurov, N. S., Abdurazakov, M., Rashidova, S. S., & Surov, O. V. (2023). Biodegradable Polyethylene-Based composites filled with cellulose Micro- and nanoparticles. Eurasian Journal of Chemistry, 28(2 (110)). https://doi.org/10.31489/2959-0663/2-23-16
[17]. 17. Solomevich, S. O., Dmitruk, E. I., Aharodnikau, U. E., Salamevich, D. A., Bychkovsky, P. M., Golub, N. V., & Yurkshtovich, T. L. (2021). Characterization of H3PO4/HNO3–$NANO_2$ oxidized bacterial cellulose and its usage as a carrier for the controlled release of cephalexin. Cellulose, *28*(14), 9425-9439. https://doi.org/10.1007/s10570-021-04130-z
[18]. 18. Lupidi, G., Pastore, G., Marcantoni, E., & Gabrielli, S. (2023). Recent developments in chemical derivatization of microcrystalline cellulose (MCC): pre-treatments, functionalization, and applications. Molecules, 28(5), 2009. https://doi.org/10.3390/molecules28052009
[19]. 19. Makhliyo, K., Abdumutolib, A., Sirojiddin, S., Nurbek, A., Khaydar, Y., & Jiang, G. (2023). Preparation of oxidized nanocellulose by using potassium dichromate. Cellulose, 30(9), 5657-5668. https://doi.org/10.1007/s10570-023-05222-8
[20]. 20. George, J., & Sabapathi, S. N. (2015). Cellulose nanocrystals: synthesis, functional properties, and applications. Nanotechnology, science and applications, 45-54. https://doi.org/10.2147/NSA.S64386
[21]. 21. Liu, H., Liu, K., Han, X., Xie, H., Si, C., Liu, W., & Bae, Y. (2020). Cellulose nanofibrils-based hydrogels for biomedical applications: progresses and challenges. Current medicinal chemistry, 27(28), 4622-4646. https://doi:10.2174/0929867327666200303102859.
[22]. 22. Gubaidullin, A. T., Makarova, A. O., Derkach, S. R., Voron'ko, N. G., Kadyirov, A. I., Ziganshina, S. A., ... & Zuev, Y. F. (2022). Modulation of molecular structure and mechanical properties of κ-carrageenan-gelatin hydrogel with multi-walled carbon nanotubes. Polymers, 14(12), 2346. https://doi.org/10.3390/polym14122346 .
[23]. 23. Kaveh, K., & Malcherek, A. (2024). Enhancing non-newtonian fluid modeling: A novel extension of the cross flow curve model. Journal of Hydro-Environment Research, 56, 17-27. https://doi.org/10.1016/j.jher.2024.08.001.
[24]. 24. Peresin, M. S., Habibi, Y., Zoppe, J. O., Pawlak, J. J., & Rojas, O. J. (2010). Nanofiber composites of polyvinyl alcohol and cellulose nanocrystals: manufacture and characterization. Biomacromolecules, 11(3), 674-681. https://doi.org/10.1021/bm901254n